

Long-term evolution of Sco X-1: implications for the current spin frequency and ellipticity of the neutron starABHIJNAN KAR,¹ PULKIT OJHA,² AND SUDIP BHATTACHARYYA³¹*Department of Physical Sciences, Indian Institute of Science Education and Research Berhampur, Vigyanpuri, Ganjam, 760003, India*²*Center for Theoretical Physics, Aleja Lotnikow 32/46, 02-668, Warszawa, Poland.*³*Department of Astronomy and Astrophysics, Tata Institute of Fundamental Research, 1 Homi Bhabha Road, Colaba, Mumbai 400005, India*

ABSTRACT

Sco X-1 is the brightest observed extra-solar X-ray source, which is a neutron star (NS) low-mass X-ray binary (LMXB), and is thought to have a strong potential for continuous gravitational waves (CW) detection due to its high accretion rate and relative proximity. Here, we compute the long-term evolution of its parameters, particularly the NS spin frequency (ν) and the surface magnetic field (B), to probe its nature and its potential for CW detection. We find that Sco X-1 is an unusually young ($\sim 7 \times 10^6$ yr) LMXB and constrain the current NS mass to $\sim 1.4 - 1.6 M_{\odot}$. Our computations reveal a rapid B decay, with the maximum current value of $\sim 1.8 \times 10^8$ G, which can be useful to constrain the decay models. Note that the maximum current ν value is ~ 550 Hz, implying that, unlike what is generally believed, a CW emission is not required to explain the current source properties. However, ν will exceed an observed cut-off frequency of ~ 730 Hz, and perhaps even the NS break-up frequency, in the future, without a CW emission. The minimum NS mass quadrupole moment (Q) to avoid this is $\sim (2 - 3) \times 10^{37}$ g cm², corresponding to a CW strain of $\sim 10^{-26}$. Our estimation of current ν values can improve the CW search sensitivity.

Keywords: Gravitational Waves (678) — Neutron stars (1108) — Low-mass x-ray binary stars (939)
— Accretion (14) — X-ray binary stars (1811)

1. INTRODUCTION

A neutron star (NS) low-mass X-ray binary (LMXB) is a binary stellar system, in which the NS accretes matter from a low-mass ($\lesssim 1.5 M_{\odot}$) donor or donor star (Bhattacharya & van den Heuvel 1991). The accretion happens when the donor fills its Roche lobe. Since this accreted matter has a large amount of specific angular momentum, it typically spins up the NS to a spin frequency (ν) of a few hundred Hz. When the accretion finally stops, i.e., at the end of the LMXB phase, such rapidly spinning NSs can manifest as radio millisecond pulsars (MSPs; Bhattacharyya & Roy 2022). Even in the LMXB phase, if the accretion disk is stopped by the NS magnetosphere, the disk matter may be channelled via accretion columns to the stellar magnetic poles. This can create azimuthally asymmetric emission from the spinning NS, and hence the observed X-ray emission can have periodic variation with the stellar spin frequency ν . Such systems are called accretion-powered millisecond X-ray pulsars (AMXPs; e.g., Patruno & Watts 2020; Salvo & Sanna 2022).

Corresponding author: Abhijnan Kar
karabhijnan123@gmail.com

pojha@cft.edu.pl

sudip@tifr.res.in

If a spinning NS is asymmetric around its spin axis, implying a nonzero ellipticity (ϵ) or mass quadrupole moment ($Q = I\epsilon$; I : NS moment of inertia), such an NS should emit gravitational waves continuously and spin down (Shapiro & Teukolsky 1983). Note that other physical mechanisms, such as r mode instability, f mode instability, etc., can also cause continuous gravitational waves (CW) emission from NS (for a comprehensive review, see Glampedakis & Gualtieri 2018). While such continuous waves (CW) have not been detected so far and only upper limits of ϵ have been estimated for a number of neutron stars (e.g., Abbott et al. 2017, 2019, 2020; Nieder et al. 2020, 2019; Whelan et al. 2023), such waves have been inferred from electromagnetic observations (e.g., Bhattacharyya & Chakrabarty 2017; Woan et al. 2018; Bhattacharyya 2020; Haskell & Patruno 2017). Studies of CW from spinning NSs can be very useful to probe their physics, formation and evolution and hence the detection of CW is a holy grail of physics and astronomy.

What are the best sources to search for CW? Among NS LMXBs, Scorpius X-1 (Sco X-1) is thought to be a very promising source for CW detection (see Mukherjee et al. 2018; Pagliaro et al. 2023, and references therein) because of its relatively low distance ($d = 2.8$ kpc; Bradshaw et al. 1999) and a very high and persistent accretion rate \dot{M} (of the order of $10^{-8} M_{\odot}\text{yr}^{-1}$; Mata Sánchez et al. 2015; Watts et al. 2008). Here is the justification for the latter argument. Such a high \dot{M} value could spin up the NS beyond the break-up ν ($\nu_{\text{break}} \gtrsim 1200$ Hz; Bhattacharyya et al. 2016), which has not obviously happened. Even if the current ν ($= \nu_{\text{curr}}$) for Sco X-1 does not exceed ν_{break} , it could exceed an observationally indicated upper cut-off of ν (~ 730 Hz; Chakrabarty et al. 2003; Chakrabarty 2008; Patruno 2010). These hint at a braking torque on the NS to keep its ν within a reasonable limit. CW can provide such a braking torque and cause the pulsar to spin down (e.g., Bhattacharyya & Chakrabarty 2017). However, in spite of this promise, the CW detection from Sco X-1 could be challenging and has not been detected yet in recent searches (Zhang et al. 2021; Whelan et al. 2023; Abbott et al. 2022a,b). This is because the source is not a pulsar and hence the ν value is not known (See Galaudage et al. 2021, and references therein). Note that a known ν_{curr} value reduces the volume of the parameter space and hence improves the sensitivity for CW searches. However, in the absence of a measured ν_{curr} value, one could estimate a range of ν_{curr} values by the computation of long-term evolution of the LMXB and reproducing other known source parameters (e.g., Kar et al. 2024). Some such parameter values of Sco X-1 are orbital period $P_{\text{orb}} = 0.787$ days (Wang et al. 2018), donor-to-NS mass ratio $q = 0.52_{-0.15}^{+0.16}$ (Wang et al. 2018), accretion rate $\dot{M} = 2.2 \times 10^{-8} M_{\odot}\text{yr}^{-1}$ (Mata Sánchez et al. 2015; Watts et al. 2008) and donor star temperature $T_{\text{donor}} < 4800$ K (Mata Sánchez et al. 2015). Such a computation is also useful to probe the binary and stellar evolution and the NS physics and to estimate other unknown parameters, including Q or ϵ . However, while a few papers, such as Chen (2017); Van & Ivanova (2019), computed the binary evolution for Sco X-1 to match some observationally known values of parameters (e.g., P_{orb} , q , \dot{M} , T_{donor}) at the current time, they did not compute and constrain most NS parameters (e.g., ν , Q).

Kar et al. (2024) explored the NS LMXB evolution, including the evolution of NS and binary parameters, for ranges of initial and fixed parameter values. Using the methods outlined in that paper, here we compute the binary evolution for Sco X-1, and for the first time, calculate the ν evolution for this source considering different Q values. Note that, unlike some previous papers (e.g., Zhang et al. 2021), we do not consider the special condition of a balance between the accretion torque and the CW torque. This condition, even if satisfied for certain periods, may not generally hold during the entire LMXB phase, and hence might not be valid at the current time. This is because the mass transfer rate from the donor star evolves drastically throughout the LMXB phase (e.g., Kar et al. 2024), and the CW may not entirely depend on accretion (e.g., Bhattacharyya 2020). Therefore, we consider the general case of the mutually independent evolution of these torques depending on the evolution of various source parameter values. Our computations constrain some NS parameters, e.g., mass (M_{NS}), ν , ϵ , surface magnetic field (B), etc., which, among various aspects, could be useful for future CW detection from Sco X-1.

2. METHODS

We use MESA¹ (Modules for Experiments in Stellar Astrophysics), an open-source 1D stellar evolution code (Paxton et al. 2011, 2013, 2015, 2018, 2019), to compute the binary evolution for Sco X-1. The binary parameter evolution and the Roche Lobe overflow (RLOF) primarily depend on the angular momentum (J) loss from the system, and the magnetic braking (MB) is the dominant mechanism for such a loss for the donor star of Sco X-1 (Van & Ivanova 2019). However, a common prescription of MB (Rappaport et al. 1983) cannot reproduce the observed high accretion rate of

¹ <https://docs.mesastar.org/en/release-r23.05.1/>

Sco X-1 and hence we use the ‘‘Convection And Rotation Boosted’’ (CARB) prescription with the loss of J due MB given by (Van & Ivanova 2019):

$$\begin{aligned} \dot{J}_{\text{MB}} = & -\frac{2}{3}\dot{M}_{\text{W}}^{-1/3}R^{14/3}(v_{\text{esc}}^2 + 2\Omega^2R^2/K_2^2)^{-2/3} \\ & \times \Omega_{\odot} B_{\odot}^{8/3} \left(\frac{\Omega}{\Omega_{\odot}}\right)^{11/3} \left(\frac{\tau_{\text{conv}}}{\tau_{\odot,\text{conv}}}\right)^{8/3}. \end{aligned} \quad (1)$$

Here, \dot{M}_{W} represents wind mass-loss rate from donor star, R is the donor star radius, v_{esc} denotes surface escape velocity of the donor star, Ω is the rotation rate, K_2 represents limit where rotation rate has significant role and τ_{conv} is convective turnover time. The other components of \dot{J} due to gravitational radiation and mass loss are considered according to their standard prescription mentioned in earlier papers (e.g., Jia & Li 2015; Goodwin & Woods 2020). However, although we primarily use the ‘‘CARB’’ magnetic braking prescription, we also run MESA, following the general results of Yang & Li (2024), for the ‘‘Convection Boosted’’ (CBOOST) magnetic braking scheme (Eq. 20 Van et al. 2019, with $\xi = 2$). For baryonic to gravitational mass conversion for the NS, we use Eq. 19 of Cipolletta et al. (2015) as outlined in Kar et al. (2024). We calculate NS radius as $R_{\text{NS}} = AM_{\text{NS}}^{1/3}$, where the value of the proportionality constant A has been determined by taking an NS radius of 11.2 km for the NS mass of 1.4 M_{\odot} .

In order to model the NS spin evolution, we follow the torque prescription in Bhattacharyya & Chakrabarty (2017) and references therein. The torques in the accretion and propeller phases (N_{acc} and N_{prop} , respectively) are

$$N_{\text{acc}} = \dot{M}\sqrt{GM_{\text{NS}}r_{\text{m}}} + \frac{\mu^2}{9r_{\text{m}}^3} \left[2\left(\frac{r_{\text{m}}}{r_{\text{co}}}\right)^3 - 6\left(\frac{r_{\text{m}}}{r_{\text{co}}}\right)^{\frac{3}{2}} + 3 \right], \quad (2)$$

$$N_{\text{prop}} = -\eta\dot{M}\sqrt{GM_{\text{NS}}r_{\text{m}}} - \frac{\mu^2}{9r_{\text{m}}^3} \left[3 - 2\left(\frac{r_{\text{co}}}{r_{\text{m}}}\right)^{3/2} \right], \quad (3)$$

where $r_{\text{m}}(\propto B^{4/7}\dot{M}^{-2/7})$ and $r_{\text{co}}(\propto \nu^{-2/3})$ are magnetospheric radius and corotation radius, respectively (e.g., Bhattacharyya & Chakrabarty 2017), μ is the NS surface magnetic dipole moment and η is a constant of the order of unity. In order to make our results realistic, we also consider that the NS surface magnetic field evolves as prescribed in Shibazaki et al. (1989):

$$B(t) = \frac{B_{\text{i}}}{1 + \Delta M_{\text{acc}}(t)/m_{\text{B}}}, \quad (4)$$

where B_{i} is the initial NS surface magnetic field, $B(t)$ is the NS surface magnetic field at time t after the accretion of $\Delta M_{\text{acc}}(t)$ mass, and m_{B} is a constant mass which determines the decay rate of the magnetic field. The current value of the NS magnetic field is B_{curr} .

Sco X-1 does not show pulsations (see section 1) and it is clearly in the accretion phase (i.e., $r_{\text{m}} \leq r_{\text{co}}$; Bhattacharyya & Chakrabarty 2017) with a high accretion rate (see Figure 1). Hence, at the current time, the NS magnetic field may be too weak to stop the accretion disk and cannot channel the accreted matter to the magnetic poles (see section 1). Therefore, we consider that the accretion disk inner radius is currently either R_{NS} or r_{ISCO} (ISCO: innermost stable circular orbit), whichever is greater (i.e., $\max[R_{\text{NS}}, r_{\text{ISCO}}]$; $r_{\text{ISCO}}(= 6GM/c^2)$, G : gravitational constant, c : speed of light in vacuum). Thus, at the current time, the lack of pulsations in the accretion phase implies that $r_{\text{m}} \not\geq \max[R_{\text{NS}}, r_{\text{ISCO}}]$ and there is no significant disk-magnetosphere interaction. Consequently, we consider $N_{\text{acc}} = \dot{M}\sqrt{GM_{\text{NS}}\max[R_{\text{NS}}, r_{\text{ISCO}}]}$ (from Eq. 2) for the current time.

For the $Q > 0$ cases, we use the following CW torque (Bildsten 1998):

$$N_{\text{CW}} = -\frac{32GQ^2}{5} \left(\frac{2\pi\nu}{c}\right)^5. \quad (5)$$

In order to calculate the CW strain (which is crucial for CW detection), we use the equation (Zimmermann & Szedenits 1979; Glampedakis & Gualtieri 2018):

$$h_0 = \frac{4\pi^2GI}{c^4d} f_{\text{CW}}^2 \epsilon, \quad (6)$$

where f_{CW} is the frequency of CW taken to be 2ν .

3. RESULTS

We consider ranges of values for initial and fixed parameters (e.g., Kar et al. 2024), such as donor star mass (M_{donor}), M_{NS} , P_{orb} , fractional loss of the mass transferred from the donor star (β), irradiation efficiency (ϵ_{irr}), for our MESA evolution models. Van & Ivanova (2019) found that the reproduction of observed Sco X-1 parameter values requires a narrow initial parameter space. Motivated by this, we consider initial ranges of M_{donor} ($1.0 - 1.2 M_{\odot}$), P_{orb} ($2.75 - 2.82$ days), M_{NS} ($1.35 - 1.6 M_{\odot}$), and also a range ($0.3 - 0.7$) of β for our computation. When we study the effects of change of one parameter value, we fix the other parameters at their canonical values (e.g., $M_{\text{NS}} = 1.4 M_{\odot}$, $M_{\text{donor}} = 1.1 M_{\odot}$, $P_{\text{orb}} = 2.80$ days, $\beta = 0.5$). Note that the values of parameters, such as ϵ_{irr} , η , do not have visible effects for our computation to reproduce Sco X-1 parameter values. By exploring the MESA evolution within the above-mentioned ranges, we find that the model with initial $P_{\text{orb}} = 2.8$ days and initial $M_{\text{donor}} = 1.1 M_{\odot}$ reproduces the observed parameter values closely (Figure 1). We match the observed values of P_{orb} , q , \dot{M} within 1% and T_{donor} within $< 5\%$, respectively. From this best model, we get $\dot{M} = 1.92 \times 10^{-8} M_{\odot} \text{yr}^{-1}$, $P_{\text{orb}} = 0.786$ days, $q = 0.596$, $T_{\text{donor}} \sim 5000$ K, all of which match most closely with the observed ranges of parameter values for Sco X-1 mentioned in Section 1. From the evolution, it can be seen that the accretion starts at $\sim 7.22 \times 10^9$ yr (Figure 1, 3). Moreover, note that the best model implies a current value of M_{NS} of $\sim 1.48 M_{\odot}$, and considering all reasonably matching evolution models, the current M_{NS} range is $\sim 1.42 - 1.6 M_{\odot}$. Figure 2 shows the Hertzsprung–Russell (HR) diagram of the evolution of donor star of Sco X-1 and its current position.

With our best model, we calculate the spin evolution and estimate the current ν value (ν_{curr}) of Sco X-1 (see Kar et al. 2024, and section 2 for details). For the default model, we keep $Q = 0$, i.e., we take a case without CW. However, with the usually considered value of m_{B} ($\sim 10^{-4} M_{\odot}$; Shibazaki et al. 1989) in Eq. 4, we cannot satisfy the condition of no pulsation in the accretion phase, viz., $r_{\text{m}} \not\geq \max[R_{\text{NS}}, r_{\text{ISCO}}]$ (see section 2). Hence, we explore a range of lower m_{B} values which allows a faster decay of NS magnetic field (Figure 3), and, in turn, provides lower B_{curr} values resulting in lower r_{m} values (e.g., Bhattacharyya & Chakrabarty 2017). We assume a reasonable lower limit of B_{curr} ($\sim 10^7$ G; see Mukherjee et al. 2015).

The conditions $r_{\text{m}} \not\geq \max[R_{\text{NS}}, r_{\text{ISCO}}]$ and $B_{\text{curr}} \gtrsim 10^7$ G provide a range of m_{B} for each B_i . We consider a reasonable B_i range of $6 \times 10^{11} - 2 \times 10^{12}$ G (e.g., Bhattacharyya & van den Heuvel 1991). This provides an overall range of m_{B} ($\sim 6 \times 10^{-7} - 2.5 \times 10^{-5}$; for our best model; Table 1). Note that, due to the above two conditions, B_{curr} has the similar range for all B_i values (upper value of $B_{\text{curr}} \sim 1.8 \times 10^8$ G; see Table 1, for example). Moreover, as indicated above, a lower m_{B} value implies a lower B_{curr} value (Table 1 and Figure 3). Besides, as B decays faster for a lower m_{B} value, the spin-up torque also decreases faster (see section 2; Eq. 2), and hence the spin-up rate is slower. Therefore, at a given time (e.g., the current time), ν is lower for lower m_{B} and B values (see Table 1 and Figure 3). However, as the range of B_{curr} does not depend on B_i , the range of ν_{curr} ($\sim 370 - 540$ Hz for the best model) also does not depend on B_i (Table 1 and Figure 3). Furthermore, we consider other evolution models, which reasonably match the Sco X-1 observed parameter values, and get similar ranges of m_{B} , B_{curr} and ν_{curr} , as mentioned above. From all of these models combined, ν_{curr} comes out to be $\sim 350 - 550$ Hz.

Let us now consider the effects of CW ($Q > 0$) on the NS spin evolution for Sco X-1. For the LMXB phase and the radio MSP phase (section 1), $\epsilon \sim 10^{-9}$ or $Q \sim 10^{36}$ g cm² for NSs has been inferred using electromagnetic observations (e.g., Woan et al. 2018; Bhattacharyya 2020). Nevertheless, we explore a Q range of $\sim 10^{36-38}$ g cm² ($\epsilon \sim 10^{-9} - 10^{-7}$), and even higher.

The effects of Q on the NS spin evolution for Sco X-1 are shown in Figure 4. Here, we consider a Q range of $\sim 10^{36-38}$ g cm², where the lower Q values are motivated by Bhattacharyya (2020). Note that $Q \geq 2.3 \times 10^{37}$ g cm² for our best model (section 3), $B_i = 6 \times 10^{11}$ G and $m_{\text{B}} = 2.5 \times 10^{-5}$ imply that ν did not and will not exceed the observationally indicated upper cut-off of ν (~ 730 Hz; section 1) throughout the LMXB phase of Sco X-1. This minimum Q is called $Q_{\text{min}(730)}$ for the above-mentioned model. If we consider a very high value of Q (e.g., 10^{40} g cm²) as the Q_{max} , then the allowed ν_{curr} range for $Q_{\text{min}(730)} - Q_{\text{max}}$ for the above-mentioned model is $\sim 500 - 70$ Hz (Figure 4). For all the matching evolution models and the allowed m_{B} range for Sco X-1, the allowed ν_{curr} range for $Q_{\text{min}(730)} - Q_{\text{max}}$ is $\sim 510 - 60$ Hz. However, for a Q range of $0 - Q_{\text{max}}$, the range of ν_{curr} for all matching models is $\sim 550 - 60$ Hz.

We calculate the current CW strain, $h_{0,\text{curr}}$, as a function of Q for Sco X-1 using Eq. 6. In order to constrain $h_{0,\text{curr}}$, we plot $h_{0,\text{curr}}$ versus Q in Figure 4b. In the same panel, we also plot ν_{curr} versus Q . Let us understand these two curves. As one gradually considers higher Q values starting from a low value, initially ν_{curr} does not decrease much when the Q values are still small (as $N_{\text{CW}} \propto Q^2$; Eq. 5). Consequently, $h_{0,\text{curr}}$ increases rapidly with Q (roughly

proportionally; Eq. 6; see Figure 4b). But, for larger Q values ($\gtrsim 10^{38}$ g cm²), ν_{curr} decreases rapidly (as $N_{\text{CW}} \propto Q^2$; Eq. 5). As a result, $h_{0,\text{curr}}$ increases slowly with Q , because $h_{0,\text{curr}} \propto \nu_{\text{curr}}^2 Q$ (Eq. 6). This means, even if the Q value of the NS in Sco X-1 is much larger than $\sim 10^{38}$ g cm², the $h_{0,\text{curr}}$ value is not significantly greater than the value for $Q \sim 10^{38}$ g cm². In fact, we do not expect an $h_{0,\text{curr}}$ value greater than a few times 10^{-26} (see Figure 4b). This points to the requirement of a minimum instrument capability for the CW detection from Sco X-1.

For the models with the magnetic braking prescription ‘‘CBOOST’’ (see section 2), we use the similar initial parameter values around the mentioned ranges for the ‘‘CARB’’ model. With this prescription too, the observed parameter values for Sco X-1 can be closely matched, except for P_{orb} which could be matched within $\sim 20\%$ at the best. The NS parameter (such as ν , B_{curr}) values calculated for ‘‘CBOOST’’ are similar to those obtained for the ‘‘CARB’’ models. For example, ν_{curr} values are within the range of $\sim 300 - 600$ Hz, which overlap with the range obtained for ‘‘CARB’’.

Table 1. Several example initial magnetic field (B_i) values and their corresponding m_B , current magnetic field (B_{curr}) and current spin frequency (ν_{curr}) ranges for Sco X-1 using evolution computations with MESA (for no CW; sections 2 and 3).

B_i (G)	m_B	B_{curr} (G)	ν_{curr} (Hz)
6×10^{11}	2.5×10^{-5}	1.81×10^8	539.8
	8×10^{-6}	5.8×10^7	451.8
	5×10^{-6}	3.62×10^7	419.8
	2×10^{-6}	1.45×10^7	375.7
8×10^{11}	1.8×10^{-5}	1.74×10^8	537.7
	8×10^{-6}	7.74×10^7	474.6
	4×10^{-6}	3.87×10^7	423.6
	1.5×10^{-6}	1.45×10^7	375.7
1×10^{12}	1.5×10^{-5}	1.81×10^8	539.8
	8×10^{-6}	9.67×10^7	492.2
	4×10^{-6}	4.83×10^7	438.6
	1.2×10^{-6}	1.45×10^7	375.7
2×10^{12}	7.5×10^{-6}	1.81×10^8	539.7
	4×10^{-6}	9.67×10^7	492.3
	1×10^{-6}	2.41×10^7	397.2
	6×10^{-7}	1.45×10^7	375.6

4. DISCUSSION AND CONCLUSION

Sco X-1 is the first discovered and the brightest observed extra-solar X-ray source. This persistent source is thought to be among the best potential sources to detect CW (section 1). Here, we compute the long-term evolution of this source to understand its nature and its potential for CW detection. Our computation of evolution of Sco X-1 using the MESA code shows that it is an unusually young NS LMXB (age $\sim 7 \times 10^6$ yr) with a predicted total LMXB lifetime of $\sim 5 \times 10^8$ yr, which is also surprisingly short (see appendix). The LMXB phase ends when the donor star does not fill its Roche lobe anymore. Moreover, the current accretion rate of the NS of Sco X-1 is rather high, which cannot be explained with a usual magnetic braking prescription and requires a boosted braking prescription, such as ‘‘CARB’’ or ‘‘CBOOST’’. While our evolution computations reproduce the known parameter values of Sco X-1, we could also constrain the current NS mass to the range $\sim 1.42 - 1.6 M_{\odot}$ (section 3). Note that mass measurement of an NS is important to probe the nature of the degenerate NS core matter at supra-nuclear densities (Bhattacharyya 2010).

We compute the NS spin frequency ν and surface magnetic field B evolution for Sco X-1 for the first time to the best of our knowledge. Here, we utilize the lack of observed pulsations from this source (see sections 1 and 2) for the first time. We find that the maximum value of the current B , i.e., of B_{curr} is $\sim 1.8 \times 10^8$ G. Thus, it is remarkable that the B value of the NS decays by at least ~ 4 orders of magnitude in just ~ 7 million years, and this fast B decay is also supported by our preferred low m_B values (section 3). Note that the physics of the B decay of NSs is a topical problem of astrophysics (Igoshev et al. 2021), and our finding should be important to constrain models. For example, the high \dot{M} could screen the magnetic field lines so well that they could not re-emerge easily. Alternatively, the Ohmic

decay could be more efficient due the high temperature because of the high \dot{M} . It is important to note that, even without CW, the current ν , i.e., ν_{curr} , value is not more than ~ 550 Hz (section 3). This value is well below both the break-up ν and the observed cut-off ν (see section 1). This means that CW from Sco X-1 is not required considering its current properties. Hence, unlike what is usually believed (see section 1), the current high \dot{M} of this source does not need CW, and hence Sco X-1 might not be one of the best sources for CW detection. Nevertheless, the source could still emit CW, and considering a Q value up to $\sim 10^{40}$ g cm², the lower limit of ν_{curr} could be ~ 60 Hz. Note that our estimation of ν_{curr} values as a function of Q can be very useful to improve the sensitivity for CW searches (see section 1). However, our evolution computations show that the ν value will exceed ~ 1200 Hz in the future, if no CW is considered (see appendix). Thus, if we assume that ν will not exceed the observed cut-off ν (see section 1) even in the future, then we need a Q of at least $\sim (2 - 3) \times 10^{37}$ g cm², implying a current CW strain h_0 , i.e., $h_{0,\text{curr}}$ of $\sim 10^{-26}$ (see section 3, Figure 4b). However, even for a very high $Q \sim 10^{40}$ g cm² (i.e., $\epsilon \sim 10^{-5}$), $h_{0,\text{curr}}$ would not be more than $\sim 7 \times 10^{-26}$ (see section 3, Figure 4b). These upper limits on $h_{0,\text{curr}}$ are somewhat comparable to those obtained from the Advanced LIGO data (e.g, [Abbott et al. 2017](#); [Whelan et al. 2023](#)).

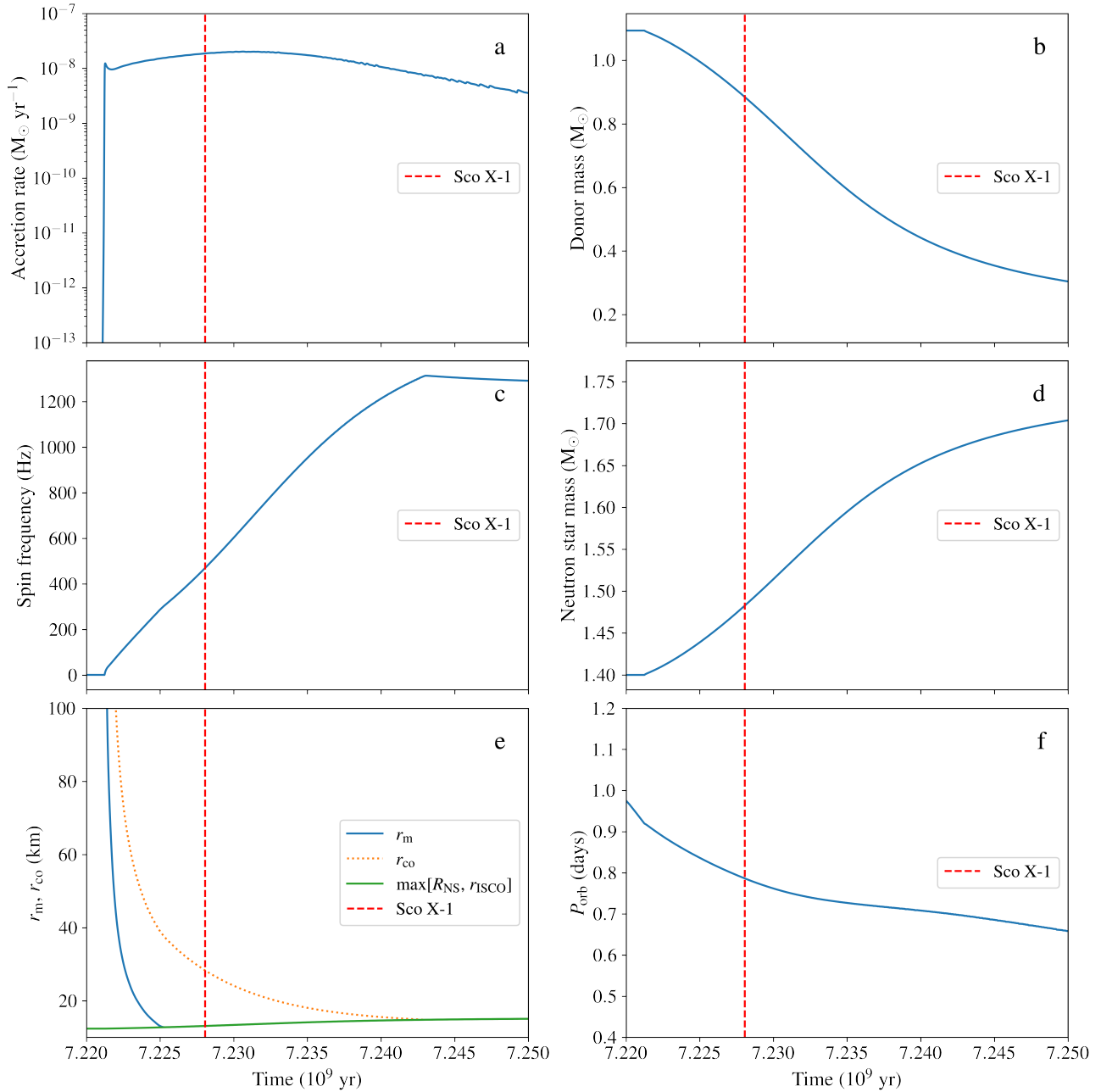


Figure 1. Evolution of parameters (accretion rate [panel a], donor star mass [panel b], NS spin frequency [panel c], NS mass [panel d], characteristic radii [panel e], and binary orbital period [panel f]) for our best model of Sco X-1 evolution as computed using MESA (section 3). The initial magnetic field (B_i) is taken to be 6×10^{11} G with $m_B = 1 \times 10^{-5}$. The dashed vertical line shows the time at which all the observed parameters of Sco X-1, P_{orb} , \dot{M} , q , T_{donor} , match. The time mentioned on the x-axis is calculated from the start of the binary evolution computation.

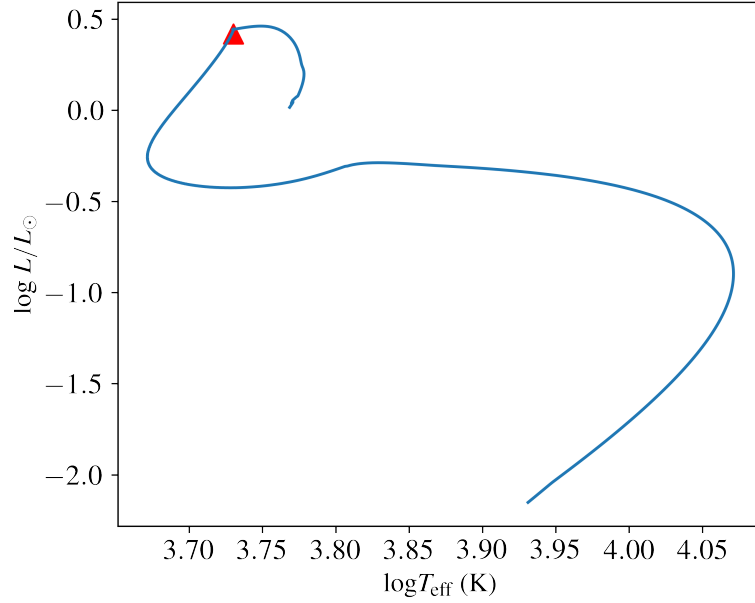


Figure 2. The HR diagram for the donor star evolution (starting from the upper end) of Sco X-1, as computed with MESA. The initial parameter values are for the best model mentioned in section 3. The current position of the source is depicted by a red triangle.

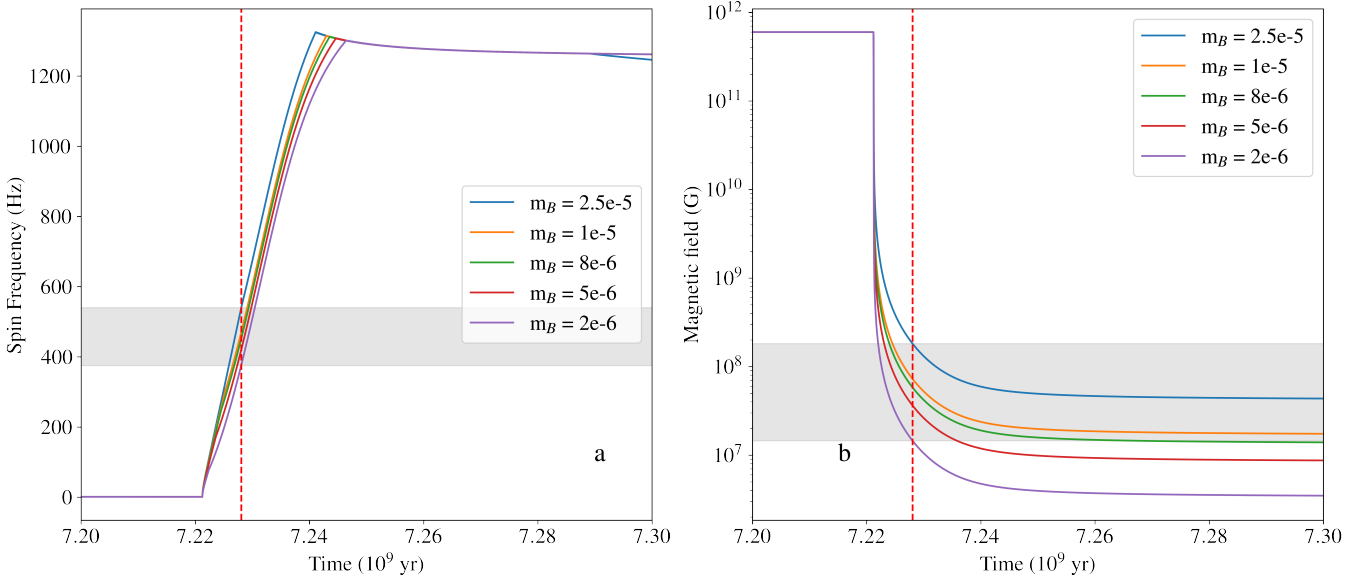


Figure 3. The evolution of the spin frequency (ν) [panel a] and the surface magnetic field (B) [panel b] of the NS of Sco X-1 for different values of m_B (Eq. 4) considering the best model mentioned in section 3. The time mentioned on the x-axis is calculated from the start of the binary evolution computation. The accretion starts at $\sim 7.22 \times 10^9$ yr which is evident from the steep rise of the ν -curve from its initial flat trajectory. The initial B is assumed to be $= 6 \times 10^{11}$ G. The dashed vertical line shows the time at which all the observed parameters of Sco X-1, P_{orb} , \dot{M} , q , T_{donor} , match. The gray patches indicate the allowed ranges of the current ν ($= \nu_{\text{curr}}$) and B ($= B_{\text{curr}}$) for the m_B values considered (see Section 3).

REFERENCES

- Abbott, B. P., Abbott, R., Abbott, T. D., et al. 2017, ApJ, 847, 47
 —. 2019, ApJ, 879, 10

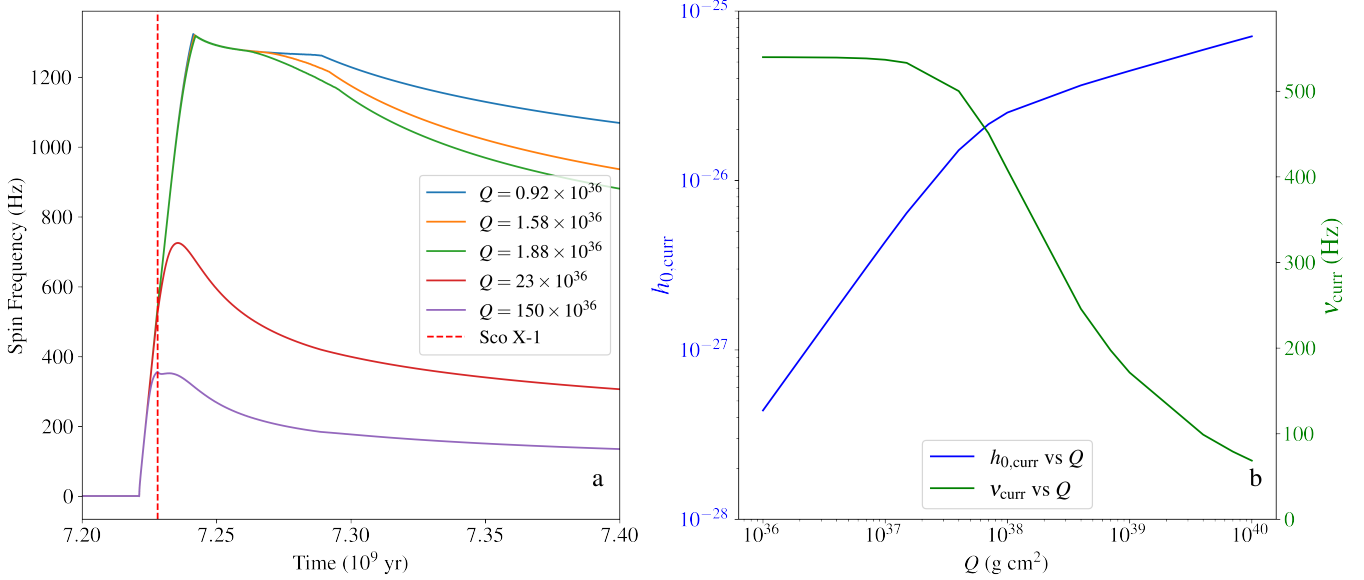


Figure 4. *Panel a:* The evolution of the NS spin frequency (ν) for Sco X-1 for different values of Q (Eq. 5) considering the best model mentioned in section 3. The time mentioned on the x-axis is calculated from the start of the binary evolution computation. The B_i and m_B values are 6×10^{11} G and 2.5×10^{-5} , respectively. The dashed vertical line shows the time at which all the observed parameters of Sco X-1, P_{orb} , \dot{M} , q , T_{donor} , match. *Panel b:* The CW strain amplitude $h_{0,\text{curr}}$ and the NS spin frequency ν_{curr} for Sco X-1 at the current time for a range of Q values (for the above-mentioned best model, B_i and m_B values; section 3). Note that $h_{0,\text{curr}}$ increases slowly beyond $Q \sim 10^{38}$ g cm 2 ($\epsilon \sim 10^{-7}$).

Abbott, R., Abbott, T. D., Abraham, S., et al. 2020, ApJL, 902, L21

Abbott, R., Abe, H., Acernese, F., et al. 2022a, Phys. Rev. D, 106, 062002

—. 2022b, ApJL, 941, L30

Bhattacharya, D., & van den Heuvel, E. 1991, Physics Reports, 203, 1

Bhattacharyya, B., & Roy, J. 2022, Radio Millisecond Pulsars, ed. S. Bhattacharyya, A. Papitto, & D. Bhattacharya (Cham: Springer International Publishing), 1–32

Bhattacharyya, S. 2010, Advances in Space Research, 45, 949

Bhattacharyya, S. 2020, MNRAS, 498, 728

Bhattacharyya, S., Bombaci, I., Logoteta, D., & Thampan, A. V. 2016, MNRAS, 457, 3101

Bhattacharyya, S., & Chakrabarty, D. 2017, ApJ, 835, 4

Bildsten, L. 1998, ApJ, 501, L89

Bradshaw, C. F., Fomalont, E. B., & Geldzahler, B. J. 1999, ApJ, 512, L121

Chakrabarty, D. 2008, AIP Conference Proceedings, 1068, 67

Chakrabarty, D., Morgan, E. H., Munro, M. P., et al. 2003, Nature, 424, 42

Chen, W.-C. 2017, A&A, 606, A60

Cipolletta, F., Cherubini, C., Filippi, S., Rueda, J. A., & Ruffini, R. 2015, Phys. Rev. D, 92, 023007

Galadage, S., Wette, K., Galloway, D. K., & Messenger, C. 2021, MNRAS, 509, 1745

Glampedakis, K., & Gualtieri, L. 2018, Gravitational Waves from Single Neutron Stars: An Advanced Detector Era Survey, ed. L. Rezzolla, P. Pizzochero, D. I. Jones, N. Rea, & I. Vidaña (Cham: Springer International Publishing), 673–736

Goodwin, A. J., & Woods, T. E. 2020, MNRAS, 495, 796

Haskell, B., & Patruno, A. 2017, Phys. Rev. Lett., 119, 161103

Igoshev, A. P., Popov, S. B., & Hollerbach, R. 2021, Universe, 7, 351

Jia, K., & Li, X.-D. 2015, ApJ, 814, 74

Kar, A., Ojha, P., & Bhattacharyya, S. 2024, MNRAS, 535, 344

Mata Sánchez, D., Muñoz-Darias, T., Casares, J., et al. 2015, MNRAS Letters, 449, L1

Mukherjee, A., Messenger, C., & Riles, K. 2018, Phys. Rev. D, 97, 043016

Mukherjee, D., Bult, P., & Michiel van der Klis, D. B. 2015, MNRAS, 452, 3994

Nieder, L., Clark, C. J., Bassa, C. G., et al. 2019, ApJ, 883, 42

Nieder, L., Clark, C. J., Kandel, D., et al. 2020, ApJL, 902, L46

Pagliaro, G., Papa, M. A., Ming, J., et al. 2023, ApJ, 952, 123

- Patruno, A. 2010, *ApJ*, 722, 909
- Patruno, A., & Watts, A. L. 2020, *Accreting Millisecond X-ray Pulsars*, ed. T. M. Belloni, M. Méndez, & C. Zhang (Springer Berlin Heidelberg), 143–208
- Paxton, B., Bildsten, L., Dotter, A., et al. 2011, *ApJS*, 192, 3
- Paxton, B., Cantiello, M., Arras, P., et al. 2013, *ApJS*, 208, 4
- Paxton, B., Marchant, P., Schwab, J., et al. 2015, *ApJS*, 220, 15
- Paxton, B., Schwab, J., Bauer, E. B., et al. 2018, *ApJS*, 234, 34
- Paxton, B., Smolec, R., Schwab, J., et al. 2019, *ApJS*, 243, 10
- Rappaport, S., Verbunt, F., & Joss, P. C. 1983, *ApJ*, 275, 713
- Salvo, T. D., & Sanna, A. 2022, *Accretion Powered X-ray Millisecond Pulsars*, ed. S. Bhattacharyya, A. Papitto, & D. Bhattacharya (Cham: Springer International Publishing), 87–124
- Shapiro, S. L., & Teukolsky, S. A. 1983 (John Wiley I& Sons, Ltd), 466–498
- Shibazaki, N., Murakami, T., Shaham, J., & Nomoto, K. 1989, *Nature*, 342, 656
- Van, K. X., & Ivanova, N. 2019, *ApJL*, 886, L31
- Van, K. X., Ivanova, N., & Heinke, C. O. 2019, *MNRAS*, 483, 5595
- Wang, L., Steeghs, D., Galloway, D. K., Marsh, T., & Casares, J. 2018, *MNRAS*, 478, 5174
- Watts, A. L., Krishnan, B., Bildsten, L., & Schutz, B. F. 2008, *MNRAS*, 389, 839
- Whelan, J. T., Tenorio, R., Wofford, J. K., et al. 2023, *ApJ*, 949, 117
- Woan, G., Pitkin, M. D., Haskell, B., Jones, D. I., & Lasky, P. D. 2018, *ApJL*, 863, L40
- Yang, H.-R., & Li, X.-D. 2024, *ApJ*, 974, 298
- Zhang, Y., Papa, M. A., Krishnan, B., & Watts, A. L. 2021, *ApJL*, 906, L14
- Zimmermann, M., & Szedenits, E. 1979, *Phys. Rev. D*, 20, 351

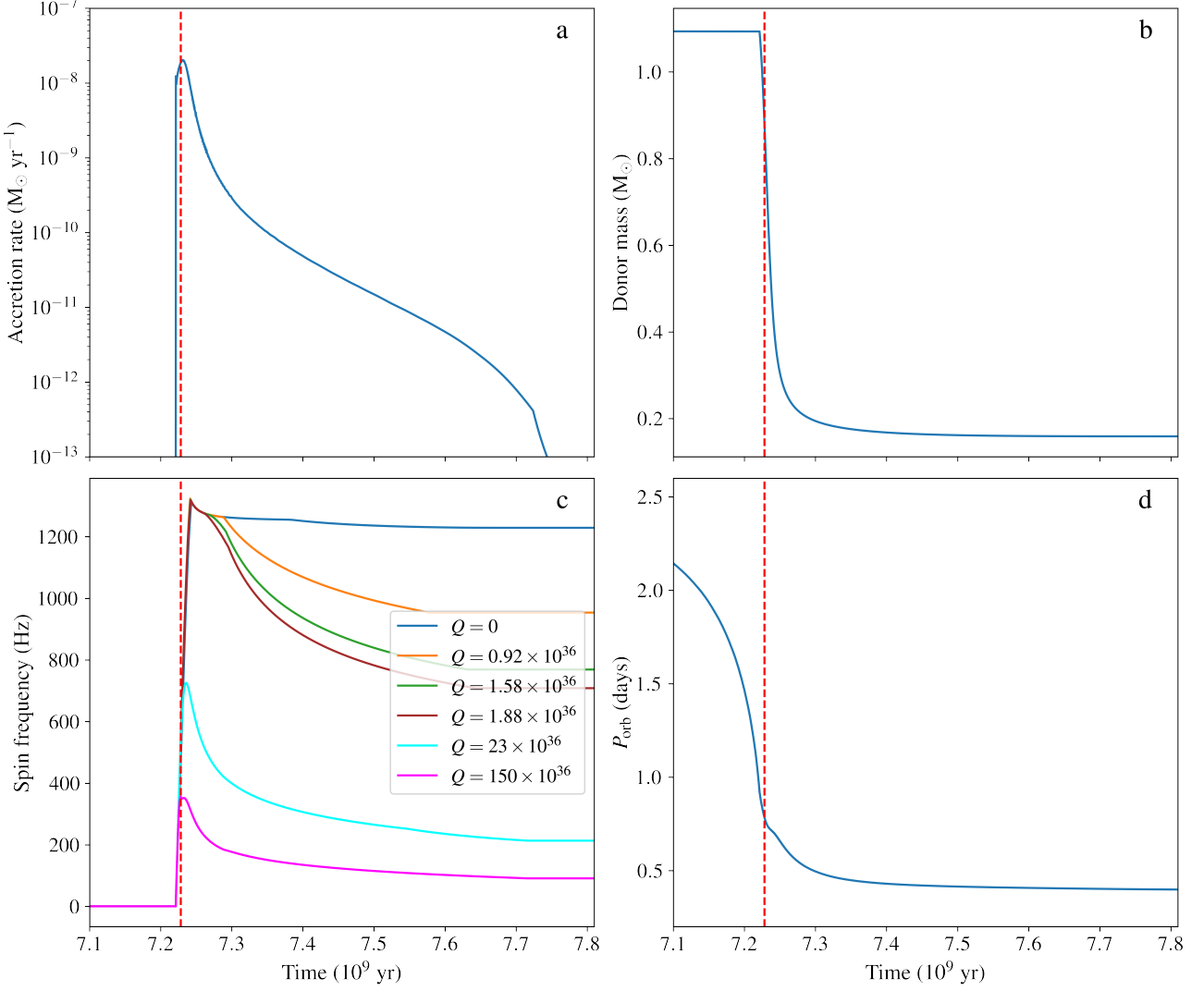


Figure A1. Evolution of parameter values, accretion rate (panel a), donor star mass (panel b), NS spin frequencies (ν for various Q values; panel c), and binary orbital period (P_{orb} ; panel d) during the entire LMXB phase for the best model of Sco X-1 (see section 3). B_i and m_B values are 6×10^{11} G and 2.5×10^{-5} , respectively. The time mentioned on the x-axis is calculated from the start of the binary evolution computation, and the dashed vertical line shows the time at which all the observed parameters of Sco X-1, P_{orb} , \dot{M} , q , T_{donor} , match. This figure shows that Sco X-1 is a relatively young NS LMXB and its LMXB phase will be relatively short-lived.

APPENDIX

Here, we show, in Figure A1, the evolution of some parameters, performed by the MESA code (see section 2), for the entire LMXB phase of Sco X-1. This is useful to understand the nature of this source, and thus, to provide a broad and general perspective of our results and conclusions.